

# Competition of coalescence and "fireball" processes in nonequilibrium emission of light charged particles from p+Au collisions

A.Budzanowski,<sup>1</sup> M.Fidelus,<sup>2</sup> D.Filges,<sup>3</sup> F.Goldenbaum,<sup>3</sup> H.Hodde,<sup>4</sup> L.Jarczyk,<sup>2</sup> B.Kamys,<sup>2,\*</sup> M.Kistryn,<sup>1</sup> St.Kistryn,<sup>2</sup> St.Kliczewski,<sup>1</sup> A.Kowalczyk,<sup>2</sup> E.Kozik,<sup>1</sup> P.Kulesa,<sup>1,3</sup> H.Machner,<sup>3</sup> A.Magiera,<sup>2</sup> B.Piskor-Ignatowicz,<sup>2,3</sup> K.Pysz,<sup>1,3</sup> Z.Rudy,<sup>2</sup> R.Siudak,<sup>1,3</sup> and M.Wojciechowski<sup>2</sup>

(PISA - Proton Induced SpAlliation collaboration)

<sup>1</sup>*H. Niewodniczański Institute of Nuclear Physics PAN, Radzikowskiego 152, 31342 Kraków, Poland*

<sup>2</sup>*M. Smoluchowski Institute of Physics, Jagellonian University, Reymonta 4, 30059 Kraków, Poland*

<sup>3</sup>*Institut für Kernphysik, Forschungszentrum Jülich, D-52425 Jülich, Germany*

<sup>4</sup>*Institut für Strahlen- und Kernphysik, Bonn University, D-53121 Bonn, Germany*

(Dated: September 17, 2021)

The energy and angular dependence of double differential cross sections  $d^2\sigma/d\Omega dE$  was measured for  $p, d, t, {}^3,4,6\text{He}, {}^{6,7,8,9}\text{Li}, {}^{7,9,10}\text{Be}$ , and  ${}^{10,11,12}\text{B}$  produced in collisions of 1.2 and 1.9 GeV protons with Au target. The beam energy dependence of these data supplemented by the cross sections from previous experiment at 2.5 GeV is very smooth. The shape of the spectra and angular distributions almost does not change in the beam energy range from 1.2 to 2.5 GeV, however, the absolute value of the cross sections increases for all ejectiles. The phenomenological model of two emitting, moving sources, with parameters smoothly varying with energy, reproduces very well spectra and angular distributions of intermediate mass fragments. The double differential cross sections for light charged particles were analyzed in the frame of the microscopic model of intranuclear cascade with coalescence of nucleons and statistical model for evaporation of particles from excited residual nuclei. However, energy and angular dependencies of data agree satisfactorily neither with predictions of microscopic intranuclear cascade calculations for protons, nor with coalescence calculations for other light charged particles. Phenomenological inclusion of another reaction mechanism - emission of light charged particles from a "fireball", i.e., fast and hot moving source - combined with the microscopic model calculations of intranuclear cascade, coalescence and evaporation of particles leads to very good description of the data. It was found that the nonequilibrium processes are very important for production of light charged particles. They exhaust 40 - 80% of the total cross sections - depending on the emitted particles. Coalescence and "fireball" emission give comparable contributions to the cross sections with exception of  ${}^3\text{He}$  data where coalescence clearly dominates. The ratio of sum of all nonequilibrium processes to those proceeding through stage of statistical equilibrium does almost not change in the beam energy range from 1.2 GeV to 2.5 GeV for all light charged particles.

PACS numbers: 25.40.-h, 25.40.Sc, 25.40.Ve

Keywords: Proton induced reactions, production of light charged particles and intermediate mass fragments, spallation, fragmentation, nonequilibrium processes, coalescence, fireball emission

## I. INTRODUCTION

In the recent publication [1] we have shown that the inclusive spectra of double differential cross sections  $d^2\sigma/d\Omega dE$  for light charged particles (LCP's) and intermediate mass fragments (IMF's) produced in proton - Au collisions at proton beam energy 2.5 GeV are compatible with the mechanism similar to cold breakup model proposed by Aichelin et al. [2]. According to this model the proton impinging on to the target drills a cylindrical hole in the nucleus what results in presence of three sources emitting LCP's, namely a small, fast, and hot "fireball" consisted of several nucleons [3], and two heavier, excited prefragments. They differ significantly in size because distribution of impact parameters favors non-central collisions which lead to asymmetric mass values of the products. Therefore, the heavier prefragment is al-

most indistinguishable from the target residuum created in microscopic models as result of the intranuclear cascade, and the lighter prefragment has typically a mass of about 20-30 nucleons. IMF's, i.e., the particles heavier than the  $\alpha$  - particle but lighter than fission fragments, cannot be emitted from the "fireball" because it consists only several nucleons, however, contributions from both heavier prefragments have been well visible in their spectra [1].

This simple picture of the reaction mechanism is very appealing because it gives a possibility to understand the presence of large nonequilibrium contribution to cross sections observed experimentally, which cannot be quantitatively reproduced by any of the existing microscopic models based on the assumption of two stages of the reaction, i.e., the fast stage consisting in intranuclear cascade of nucleon-nucleon collisions - described by INC, BUU or QMD models, and the slow stage of reaction in which heavy target residuum reaches statistical equilibrium and evaporates particles - described by statistical models.

It should be pointed out, that phenomenological anal-

---

\*Electronic address: ufkamys@cyf-kr.edu.pl

ysis published in our previous work is not able to unambiguously distinguish processes proceeding through phase of statistical equilibrium of heavy target residuum from reactions in which a nonequilibrium mechanism, i.e., the fast breakup of the target, produces heavy, excited pre-fragment moving slowly and therefore being almost indistinguishable from the target residuum.

To get more insight into the reaction mechanism it is necessary to investigate energy dependence of the reaction processes as well as to study interaction of protons with various targets. A goal of the present work was to examine beam energy dependence of the emission of LCP's and IMF's from the collisions of protons with Au target in a broad proton energy range - from 1.2 GeV to 2.5 GeV. For this purpose new experimental data were measured and analyzed, confronted whenever possible with a microscopic description of the data instead of pure phenomenological treatment as in Ref. [1].

Experimental data are discussed in the next section, the theoretical analysis is described in the third section, discussion of obtained results is presented in the fourth section, and summary of results is given in the last section.

## II. EXPERIMENTAL DATA

The experiment was performed with the selfsupporting Au target of the thickness of about of  $300 \mu\text{g}/\text{cm}^2$ , irradiated by internal proton beam of COSY (COoler SYnchrotron) of the Jülich Research Center. The experimental setup and procedure of data taking were in details described in Refs. [1] and [4]. Thus, here we only point out that the operation of the beam was performed in so called supercycle mode, i.e. alternating for each requested beam energy several cycles, consisting of protons injection to COSY ring, their acceleration with the beam circulating below the target, and irradiation of the target. Due to this all experimental conditions; setup, electronics, the target thickness and its position were exactly the same for all three studied proton energies - 1.2, 1.9 and 2.5 GeV. In this way the energy dependence was not biased by systematic effects caused by possible modifications of the experimental conditions for experiments with different beam energy.

Double differential cross sections  $d^2\sigma/d\Omega dE$  were measured as a function of scattering angle and energy of ejectiles, which were mass and charge identified for isotopes of H, He, Li, Be, and B. Heavier ejectiles i.e. C, N, O, F, Ne, Na, Mg, and Al were only charge identified. Typical spectra of isotopically identified ejectiles obtained in the present experiment are shown in Fig. 1. As can be seen in this figure the shape of spectra does not vary significantly with beam energy. The main effect, present for all products is monotonic increase of the absolute value of the cross sections with beam energy. Furthermore, all the spectra contain two components; low energy component of the Gaussian shape - attributed to evaporation from

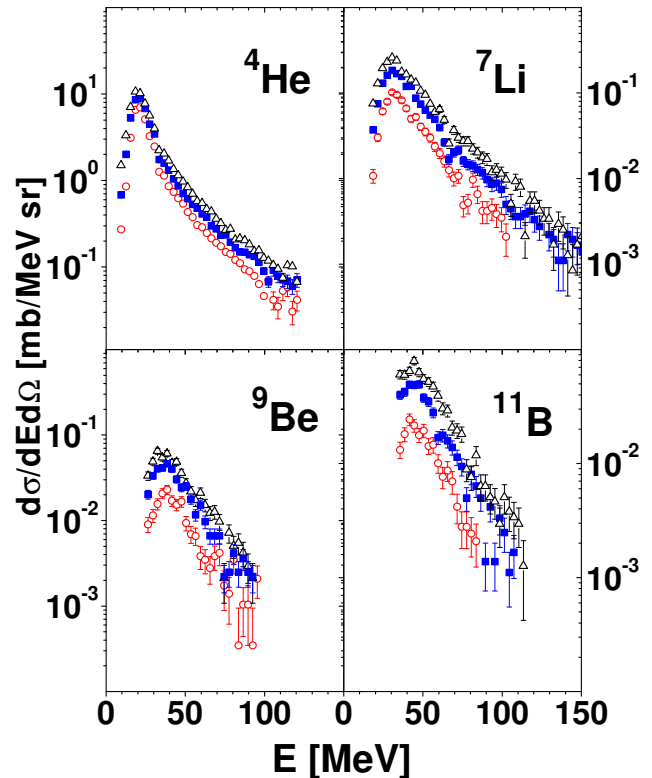


FIG. 1: (Color online) Typical spectra of  ${}^4\text{He}$ ,  ${}^7\text{Li}$ ,  ${}^9\text{Be}$ , and  ${}^{11}\text{B}$  ejectiles (upper left, upper right, lower left, and lower right parts of the figure, respectively) measured at  $35^\circ$  for three energies of the proton beam; 1.2, 1.9, and 2.5 GeV, impinging on to the Au target. Open circles represent the lowest energy, full squares - the intermediate energy, whereas open triangles show the data for the highest energy. The cross sections at 2.5 GeV proton beam energy were published in Ref. [1] and the data at 1.2 and 1.9 GeV were obtained in the present experiment.

an equilibrated, excited nucleus, and high energy exponential component - interpreted as nonequilibrium mechanism contribution. The data for LCP's, represented in Fig. 1 by  $\alpha$ -particles, have similar character and energy dependence as those for IMF's, however, the nonequilibrium component is more pronounced.

## III. THEORETICAL ANALYSIS

The equilibrium emission of LCP's and IMF's may be portrayed by statistical model of particle evaporation from excited heavy target residuum created in the fast stage of the reaction. This is, however, not the case for nonequilibrium emission of composite particles, which cannot be satisfactorily described by models used for reproduction of the first stage of the reaction, i.e., by intranuclear cascade, Boltzmann-Uehling-Uhlenbeck

or Quantum Molecular Dynamics models. All mentioned models of the reaction neglect to large extent possible multinucleon correlations, which can be crucial for nonequilibrium processes. Whereas it is possible to take effectively these correlations into account for LCP's - by introducing coalescence of emitted nucleons into clusters - such a procedure is not sufficient for description of IMF's nonequilibrium emission. From this reason different theoretical analysis has been performed for LCP's and for IMF's.

The IMF's data have been analyzed in the frame of phenomenological model of two moving sources as it was done for the data measured at 2.5 GeV beam energy in the previous investigation of these reactions [1]. In this way the energy dependence of IMF's production could be studied in a consistent way. This analysis is described in subsection III A.

The LCP's nonequilibrium emission can be, on the contrary, analyzed in the frame of the microscopic model, which assumes that the mechanism of nonequilibrium reactions consists in intranuclear cascade of nucleon-nucleon collisions [5] accompanied by coalescence of the nucleons escaping from the nucleus as it was done in Refs. [6],[7]. The authors of these papers claimed that the main properties of nonequilibrium emission of LCP's are well reproduced by the proposed microscopic model. Thus, in the present study the INCL4.3 computer program [7] has been used for description of the intranuclear cascade of nucleon-nucleon collisions with inclusion of coalescence of nucleons, whereas the GEM2 computer program [9],[10] served for evaluation of evaporation of particles from heavy target residuum remaining after the intranuclear cascade. It was also investigated whether eventual disagreement of the microscopic model calculations with experimental results leaves still a room for contribution from another mechanism, namely the "fire-ball" emission postulated in our previous paper [1]. This analysis is described in subsection III B.

### A. Intermediate mass fragments

The main assumptions of the phenomenological model of two moving sources have been formulated in the paper of Westfall *et al.* [8]. They consist in description of double differential cross sections  $d^2\sigma/d\Omega dE$  as incoherent sum of contributions originating from isotropic emission of particles from two sources moving in direction parallel to the beam direction. Each of the sources has Maxwellian distribution of the energy available for the two body decay resulting in emission of the detected particles. Velocity of the source -  $\beta$ , its temperature -  $T$ , and contribution to the total production cross section -  $\sigma$  are treated as free parameters. The presence of the Coulomb barrier which hinders emission of low energy particles was originally taken into account by energy sharp cut off, smoothed in turn by weighting with uniform or Gaussian probability distribution of the height of the bar-

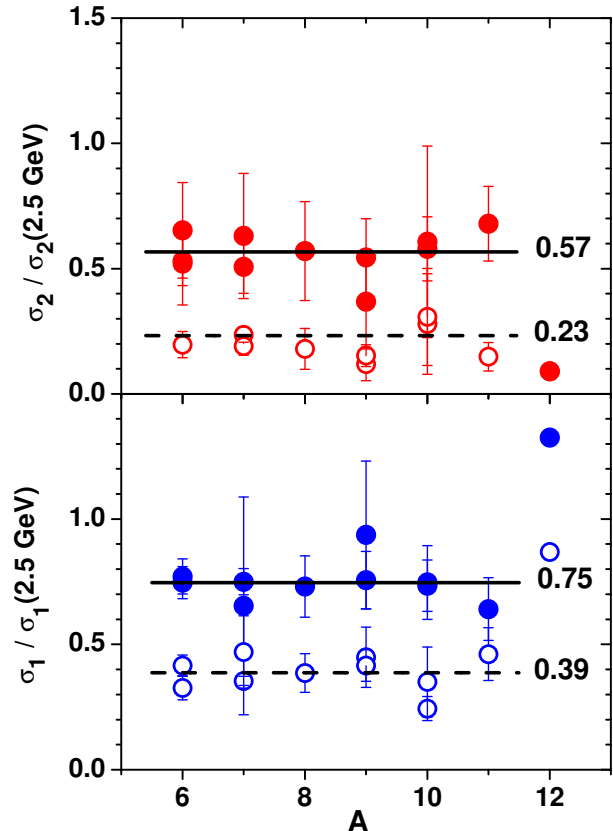


FIG. 2: (Color online) Symbols  $\sigma_1$  and  $\sigma_2$  correspond to slow and fast emitting source, respectively. Full dots represent ratio of production cross sections at beam energy 1.9 GeV to those found at 2.5 GeV as a function of mass of emitted IMF's. Open circles depict such a ratio for cross sections measured at 1.2 GeV to those determined at 2.5 GeV. The lines, present in the figure show average values of the ratios: 0.23, and 0.57 for the fast source at 1.2 GeV, and 1.9 GeV, respectively, as well as 0.39, and 0.75 for the slow source at these energies.

rier. In our recent paper [1] we used another method, namely we multiplied the Maxwellian energy distribution by smooth function corresponding to transmission probability through the barrier. Presence of Coulomb barrier introduces two parameters which influence mainly low energy part of the spectra:  $k$ -parameter, i.e., height of the Coulomb barrier in units of the height of barrier  $B$  of two charged, touching spheres of radius  $1.44 A^{1/3}$ ;  $B = Z_1 Z_2 e^2 / 1.44 (A_1^{1/3} + A_2^{1/3})$ , and ratio  $B/d$ , where  $d$  is a diffuseness of the transmission function through the barrier:  $P(E) = (1 + \exp((E - kB)/d))^{-1}$ . Details of this procedure, as well as interpretation of parameters of the model can be found in Appendix of Ref. [1].

The parameters of two moving sources were fitted to experimental data consisted of energy spectra measured at seven angles:  $16^\circ$ ,  $20^\circ$ ,  $35^\circ$ ,  $50^\circ$ ,  $65^\circ$ ,  $80^\circ$ , and  $100^\circ$ . To decrease the number of parameters it was assumed

TABLE I: Parameters of two moving sources for isotopically identified IMF's:  $k$ ,  $\beta$ ,  $T$ , and  $\sigma$  correspond to reduced height of the Coulomb barrier for emission of fragments (see the text for the explanation), source velocity, its apparent temperature, and total (integrated over angle and energy of detected particles) production cross section, respectively. The left part of the Table (parameters with indices "1") corresponds to the slow moving source, and the right part of the Table I contains values of parameters for the fast moving source. The upper row for each ejectile corresponds to beam energy 1.2 GeV, the intermediate row to 1.9 GeV, and the lowest one to the energy 2.5 GeV. Velocities for slow sources are fixed at value 0.003c estimated as velocities of heavy target residua from intranuclear cascade calculations.

| Ejectile           | Slow source     |                  |                      | Fast source     |                   |                  |                      | $\chi^2$ |
|--------------------|-----------------|------------------|----------------------|-----------------|-------------------|------------------|----------------------|----------|
|                    | $k_1$           | $T_1/\text{MeV}$ | $\sigma_1/\text{mb}$ | $k_2$           | $\beta_2$         | $T_2/\text{MeV}$ | $\sigma_2/\text{mb}$ |          |
| ${}^6\text{He}$    | $0.97 \pm 0.09$ | $9.3 \pm 1.1$    | $8.1 \pm 1.1$        | $0.47 \pm 0.05$ | $0.034 \pm 0.007$ | $13.6 \pm 1.2$   | $3.9 \pm 1.0$        | 2.7      |
|                    | $0.95 \pm 0.04$ | $9.1 \pm 0.6$    | $18.5 \pm 1.2$       | $0.36 \pm 0.05$ | $0.040 \pm 0.007$ | $19.1 \pm 1.3$   | $4.9 \pm 1.1$        | 2.6      |
|                    | $0.97 \pm 0.04$ | $9.0 \pm 0.6$    | $24.8 \pm 1.4$       | $0.35 \pm 0.05$ | $0.040 \pm 0.007$ | $21.6 \pm 1.4$   | $7.5 \pm 1.4$        | 2.1      |
| ${}^6\text{Li}$    | $0.89 \pm 0.05$ | $12.4 \pm 0.9$   | $10.5 \pm 0.8$       | $0.43 \pm 0.08$ | $0.047 \pm 0.008$ | $22.2 \pm 1.3$   | $2.85 \pm 1.3$       | 2.4      |
|                    | $0.85 \pm 0.04$ | $12.1 \pm 0.7$   | $19.5 \pm 1.2$       | $0.43 \pm 0.05$ | $0.040 \pm 0.004$ | $23.6 \pm 0.7$   | $7.7 \pm 1.1$        | 2.4      |
|                    | $0.86 \pm 0.04$ | $11.1 \pm 0.8$   | $25.3 \pm 1.7$       | $0.44 \pm 0.04$ | $0.034 \pm 0.003$ | $23.7 \pm 0.6$   | $14.5 \pm 1.7$       | 2.0      |
| ${}^7\text{Li}$    | 0.89            | 12.3             | 18.0                 | 0.47            | 0.039             | 16.4             |                      | 4.8      |
|                    | $0.88 \pm 0.03$ | $11.7 \pm 0.5$   | $38.1 \pm 1.8$       | $0.37 \pm 0.04$ | $0.040 \pm 0.005$ | $20.3 \pm 0.7$   | $10.3 \pm 1.7$       | 4.2      |
|                    | $0.88 \pm 0.03$ | $11.6 \pm 0.6$   | $50.8 \pm 2.6$       | $0.36 \pm 0.03$ | $0.035 \pm 0.003$ | $20.9 \pm 0.5$   | $20.3 \pm 2.6$       | 3.1      |
| ${}^8\text{Li}$    | $0.94 \pm 0.11$ | $11.1 \pm 1.6$   | $3.51 \pm 0.45$      | $0.48 \pm 0.08$ | $0.040 \pm 0.008$ | $14.4 \pm 2.0$   | $1.15 \pm 0.45$      | 1.8      |
|                    | $0.90 \pm 0.08$ | $11.8 \pm 1.3$   | $6.65 \pm 0.90$      | $0.43 \pm 0.05$ | $0.032 \pm 0.006$ | $17.2 \pm 1.1$   | $3.65 \pm 0.93$      | 2.5      |
|                    | $0.90 \pm 0.09$ | $11.9 \pm 1.5$   | $9.1 \pm 1.4$        | $0.45 \pm 0.05$ | $0.029 \pm 0.005$ | $18.0 \pm 1.0$   | $6.4 \pm 1.5$        | 2.1      |
| ${}^9\text{Li}$    | $1.01 \pm 0.19$ | $11.9 \pm 2.9$   | $0.92 \pm 0.09$      | $0.58 \pm 0.33$ | $0.044 \pm 0.008$ | $4.1 \pm 1.8$    | $0.25 \pm 0.12$      | 1.1      |
|                    | $0.84 \pm 0.09$ | $10.4 \pm 3.0$   | $1.92 \pm 0.37$      | $0.51 \pm 0.08$ | $0.034 \pm 0.008$ | $11.9 \pm 2.5$   | $0.77 \pm 0.33$      | 1.5      |
|                    | $1.00 \pm 0.22$ | $10.4 \pm 3.0$   | $2.1 \pm 0.5$        | $0.39 \pm 0.07$ | $0.025 \pm 0.003$ | $18.2 \pm 1.6$   | $2.1 \pm 0.6$        | 1.2      |
| ${}^7\text{Be}$    | 0.89            | 13.3             | 1.22                 | 0.52            | 0.036             | 25.3             | 0.88                 | 1.1      |
|                    | $0.86 \pm 0.21$ | $14.1 \pm 5.3$   | $1.7 \pm 1.0$        | $0.61 \pm 0.06$ | $0.025 \pm 0.007$ | $22.8 \pm 1.2$   | $2.9 \pm 1.0$        | 1.2      |
|                    | $0.92 \pm 0.27$ | $11.2 \pm 4.3$   | $2.6 \pm 0.8$        | $0.48 \pm 0.05$ | $0.038 \pm 0.005$ | $24.0 \pm 1.2$   | $4.6 \pm 0.9$        | 1.4      |
| ${}^9\text{Be}$    | 0.86            | 9.7              | 5.2                  | 0.50            | 0.030             | 15.2             | 1.24                 | 1.7      |
|                    | 0.88            | 9.8              | 9.5                  | 0.59            | 0.022             | 15.0             | 4.41                 | 1.4      |
|                    | $0.86 \pm 0.12$ | $9.6 \pm 1.7$    | $12.5 \pm 1.9$       | $0.53 \pm 0.06$ | $0.020 \pm 0.005$ | $16.6 \pm 0.8$   | $8.1 \pm 2.3$        | 1.4      |
| ${}^{10}\text{Be}$ | $0.86 \pm 0.16$ | $12.4 \pm 2.1$   | $3.5 \pm 1.3$        | $0.62 \pm 0.14$ | $0.024 \pm 0.011$ | $9.0 \pm 3.7$    | $1.9 \pm 1.3$        | 1.8      |
|                    | 0.86            | 12.0             | 7.34                 | 0.47            | 0.027             | 13.3             | 13.3                 | 1.8      |
|                    | $0.90 \pm 0.08$ | $11.8 \pm 1.2$   | $10.0 \pm 1.4$       | $0.44 \pm 0.04$ | $0.026 \pm 0.004$ | $14.5 \pm 0.9$   | $6.8 \pm 1.5$        | 1.3      |
| ${}^{10}\text{B}$  | 0.83            | 11.7             | 1.61                 | 0.78            | 0.017             | 15.9             | 0.83                 | 2.8      |
|                    | 0.87            | 10.2             | 4.93                 | 0.70            | 0.021             | 17.7             | 1.64                 | 1.5      |
|                    | $0.85 \pm 0.20$ | $10.5 \pm 3.4$   | $6.6 \pm 1.3$        | $0.73 \pm 0.14$ | $0.020 \pm 0.010$ | $18.2 \pm 2.7$   | $2.7 \pm 1.7$        | 1.8      |
| ${}^{11}\text{B}$  | $0.84 \pm 0.11$ | $10.6 \pm 1.4$   | $5.9 \pm 0.7$        | $0.53 \pm 0.08$ | $0.032 \pm 0.008$ | $10.6 \pm 2.2$   | $1.9 \pm 0.6$        | 0.94     |
|                    | 0.90            | 10.2             | 8.2                  | 0.57            | 0.019             | 13.9             | 8.7                  | 1.6      |
|                    | $0.93 \pm 0.18$ | $10.5 \pm 2.1$   | $12.8 \pm 2.5$       | $0.50 \pm 0.05$ | $0.022 \pm 0.004$ | $14.5 \pm 0.7$   | $12.8 \pm 2.8$       | 1.7      |
| ${}^{12}\text{B}$  | 0.83            | 11.9             | 1.39                 | 0.54            | [0.032]           | 12.5             | 0.46                 | 1.3      |
|                    | 0.88            | 7.8              | 2.12                 | 0.71            | 0.017             | 13.5             | 2.57                 | 1.2      |
|                    | 0.87            | 8.8              | 1.6                  | 0.73            | 0.012             | 13.2             | 5.1                  | 1.0      |

that velocity of the slow source emitting IMF's is equal to velocity of the heavy residuum from intranuclear cascade, i.e.,  $\beta_1=0.003$ . Variation of this velocity influences very slightly values of other parameters, e.g., its modification by 30% causes changes of other parameters smaller than their errors estimated by fitting computer program. Furthermore, the  $B/d$  ratio was arbitrarily assumed to be equal to 5.5. In evaluation of  $k$ -parameter it was assumed that  $B$  is defined as the Coulomb barrier between the emitted particles and the target nucleus. This assumption allows for easy comparison of  $k$ -parameter values for different ejectiles and emitting sources.

The computer program searching for the best fit values of the parameters was able in most cases to provide estimation of errors of the parameters. However, sometimes this was not possible, especially when strong ambiguities

of parameters were present. Therefore, some values of the parameters are quoted without estimation of errors. In this case it may happen that the accuracy of determination of this parameters is poorer than that for the parameters accompanied by estimates of errors.

Very good description of the spectra of all IMF's has been obtained as can be judged from  $\chi^2$  values quoted in the Table I, which vary usually between 1 and 2.

As can be seen from the Table I, values of the parameters found from the fit to the data obtained at 1.2 and at 1.9 GeV are very close to those which were determined in the analysis of the data at 2.5 GeV beam energy. This is not true for the total cross sections which increase monotonically with energy for both emitting sources. This increase is illustrated by Fig. 2 where ratios of the total cross sections found for data at 1.2 GeV, and at 1.9 GeV

to cross sections found for data at 2.5 GeV are shown as open circles and full dots respectively. The ratios of total cross sections for the fast source are shown in the upper part of the figure and those for the slow source are depicted in the lower part of the figure. The following conclusions can be derived from inspection of Fig. 2 :

- (i) The ratios of the cross sections for both sources  $\sigma_1(E, A)/\sigma_1(2.5\text{GeV}, A)$  and  $\sigma_2(E, A)/\sigma_2(2.5\text{GeV}, A)$  are independent of the mass  $A$  of ejectiles (with exception of the  $^{12}\text{B}$  cross sections, which are, however, not well determined because of poor statistics of the data).
- (ii) Cross sections for both sources are always larger for  $E=1.9$  GeV than cross sections for  $E=1.2$  GeV (full dots are above open circles) and cross sections for  $E=2.5$  GeV are the largest (the ratios are always smaller than unity).
- (iii) The averaged over mass of ejectiles ratios of the cross sections for the slow source, i.e.  $\langle \sigma_1(1.2 \text{ GeV}) / \sigma_1(2.5 \text{ GeV}) \rangle = 0.39$ , and  $\langle \sigma_1(1.9 \text{ GeV}) / \sigma_1(2.5 \text{ GeV}) \rangle = 0.75$ , are larger than the corresponding ratios for the fast source, i.e.  $\langle \sigma_2(1.2 \text{ GeV}) / \sigma_2(2.5 \text{ GeV}) \rangle = 0.23$ , and  $\langle \sigma_2(1.9 \text{ GeV}) / \sigma_2(2.5 \text{ GeV}) \rangle = 0.57$ . This means that the cross sections of the slow source increase relatively slower in the beam energy range from 1.2 GeV to 2.5 GeV than the cross sections attributed to the fast source, thus the contribution from the fast source becomes more important for higher beam energy. This is confirmed by the fact, that the relative contribution  $\sigma_2(E, A)/(\sigma_1(E, A) + \sigma_2(E, A))$  of the fast source to the total production cross section of IMF's, evaluated using the numbers from the Table I, increases with energy in almost the same way for all IMF's. In average, this contribution is equal to  $0.27 \pm 0.03$ ,  $0.33 \pm 0.05$ , and  $0.44 \pm 0.05$  for beam energy equal to 1.2, 1.9, and 2.5 GeV, respectively.

The above findings are also illustrated by Fig. 3 in which energy dependence of cross sections  $\sigma_1$  and  $\sigma_2$  is shown for emission from the slow source and fast source, respectively, as well as energy dependence of the relative contribution of the fast source  $\sigma_2$  to the total cross section  $\sigma_1 + \sigma_2$ . Note using of different scales; linear for the upper part of the figure, and logarithmic for the middle and lower parts of the figure. It may be observed, that  $\sigma_1$  and  $\sigma_2$ , vary rather fast with energy;  $\sigma_1$  increases  $\sim 2$ -3 times in the studied energy range whereas  $\sigma_2$  increases even more, i.e.,  $\sim 3$ -5 times. However the relative contribution of nonequilibrium mechanism, i.e.,  $\sigma_2/(\sigma_1 + \sigma_2)$  increases much slower, as it was mentioned above, because of the same energy trend for both cross sections  $\sigma_1$  and  $\sigma_2$ .

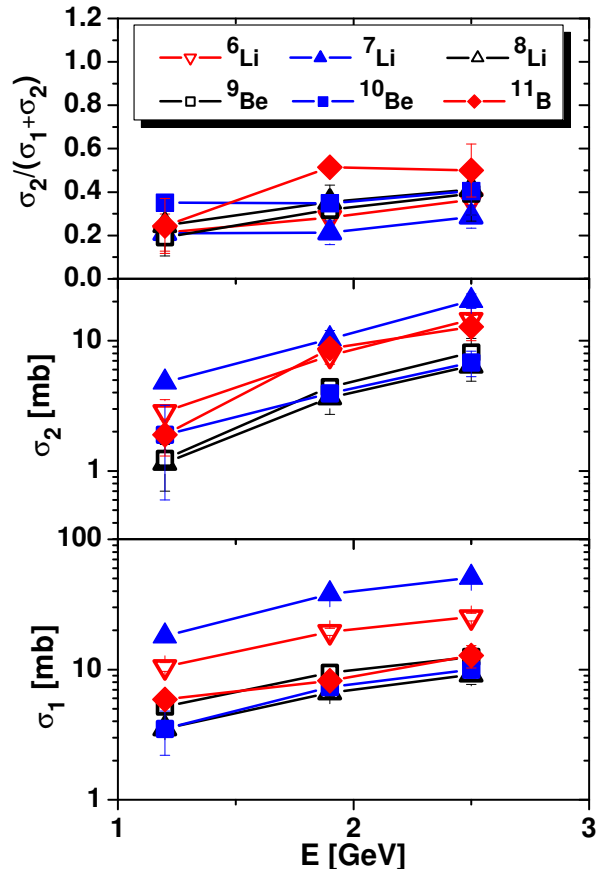


FIG. 3: (Color online) Energy dependence of the cross section  $\sigma_1$ , corresponding to emission from the slow source, is shown in the lower part of the figure, energy dependence of the cross section  $\sigma_2$ , related to emission from the fast source, is depicted in the middle part of the figure, whereas energy dependence of the relative contribution of the fast source is presented in the upper part of the figure.

## B. Light charged particles

It is well known that the cross sections for production of LCP's are at least order of magnitude larger than cross sections for emission of IMF's. Therefore, knowledge of the mechanism of LCP's production is crucial for understanding of the full interaction process. The coalescence mechanism seems to be very promising for explanation of nonequilibrium production of LCP's [6],[7]. However, it is obvious, that such a hypothesis relies on the proper reproduction of the nucleon spectra by intranuclear cascade mechanism. In the case of lack of good description of the proton spectra, the coalescence mechanism cannot alone be responsible for the observed nonequilibrium emission of LCP's. To study importance of the coalescence in the production of LCP's, the experimental proton spectra for three studied energies were compared with predictions of

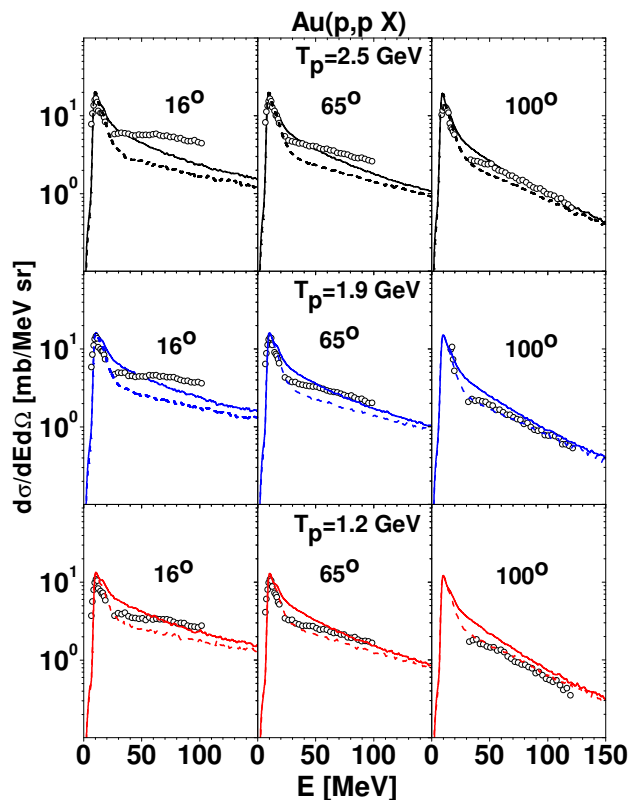


FIG. 4: (Color online) Open circles represent experimental energy spectra of protons measured at selected angles:  $16^\circ$ ,  $65^\circ$ , and  $100^\circ$  (left, central, and right column of the figure, respectively) for three proton beam energies: 1.2, 1.9 GeV – present experiment, and 2.5 GeV – Ref. [1] (lower, central, and upper row of the figure, respectively). The solid lines show results of calculations performed in the frame of intranuclear cascade formalism by means of INCL4.3 program [7] combined with the evaporation of protons from excited residual nuclei after fast stage of the reaction evaluated by means of the GEM2 program of S. Furihata [9],[10]. The dashed lines present calculations made also with INCL4.3 plus GEM2 programs, however, the coalescence of nucleons into light complex particles is taken into account according to prescription proposed in Ref. [7].

the intranuclear cascade model coupled with evaporation of nucleons. The calculations have been performed by means of INCL4.3 computer program [7] in which coalescence of nucleons can be taken optionally into account, whereas evaporation of protons as well as complex particles was described by GEM2 computer program [9],[10].

Such calculations, done with inclusion of coalescence and without this mechanism, are presented in Fig. 4 as dashed and solid lines, respectively, together with experimental proton spectra - circles.

As can be seen, the theoretical spectra obtained from calculations neglecting the coalescence overestimate the experimental spectra at proton beam energy of 1.2 GeV,

but underestimate big part of the spectra at beam energy of 2.5 GeV in particular for most forward angles. It seems, that the theoretical proton spectra evaluated without coalescence have different beam energy dependence than the experimental data. Inclusion of coalescence significantly decreases the theoretical cross sections for protons, what causes that theoretical spectra are below the experimental data for all beam energies and for all scattering angles. The height of the evaporation peak is slightly overestimated in both types of the calculations.

Further inspection of Fig. 4 leads to the conclusion that there are two obvious trends in the difference of the theoretical spectra evaluated with the coalescence mechanism and the experimental data: (i) The higher the beam energy, the larger the underestimation of the high energy part of the data by theory, and (ii) the smaller the scattering angle in respect to the proton beam direction, the larger underestimation of the data. This effects might be explained by the assumption, that an additional process exists, which manifests itself mainly at small scattering angles and gives increasing contribution to the emission of protons for larger beam energies. Such a contribution can correspond to the presence of the "fireball" emission, which due to fast motion in forward direction should modify the cross sections mainly at forward scattering angles. However, in the microscopic calculations performed according to intranuclear cascade model there is no explicit room for such a process. Therefore, inclusion of "fireball" emission should be automatically accompanied by decreasing the contribution from direct processes simulated by intranuclear cascade and coalescence of escaping nucleons. According to the reasoning given to above, the spectra of protons evaluated from intranuclear cascade with inclusion of coalescence and with contribution of evaporation of particles were multiplied by a factor, common for all scattering angles, treated as a free parameter of the fit and then added to the contribution from the "fireball" emission calculated according to the formula of single moving source emitting isotropically the LCP's [8]. The parameters of the single moving source - the "fireball", i.e. its temperature parameter -  $T$ , velocity of the source -  $\beta$ , total production cross section associated with this mechanism -  $\sigma$  was treated also as free parameters. Height of the Coulomb barrier between the "fireball" and emitted ejectile was arbitrarily fixed at 2 % of the estimated Coulomb barrier for emission from the target nucleus. Values of the parameters of "fireball" are given in the Table II.

The fit was performed for 7 scattering angles ( $16^\circ$ ,  $20^\circ$ ,  $35^\circ$ ,  $50^\circ$ ,  $65^\circ$ ,  $80^\circ$ , and  $100^\circ$ ). Results of the fit are presented in Fig. 5 for 3 angles, the smallest, the intermediate and the largest, where the dashed lines show contribution of intranuclear cascade with surface coalescence and evaporation, the dash-dotted lines present contribution from "fireball" emission, and the solid line depicts sum of both contributions. As can be seen the excellent agreement could be obtained for all scattering angles and beam energies. It is worth to emphasize, that the "fire-

TABLE II: Parameters of the "fireball":  $\beta$ ,  $T$ , and  $\sigma$  correspond to "fireball" velocity, its apparent temperature, and total (integrated over angle and energy of detected particles) production cross section, respectively,  $B/d$  determines the ratio of the threshold energy for emission of the particles (height of the Coulomb barrier) to diffuseness of the transmission function through the barrier. Parameter  $F$  is the scaling factor of coalescence and evaporation contribution extracted from fit to the proton spectra. The numbers in parentheses show fixed values of the parameters. Note, that for  $\alpha$  particles additional moving source should be added with parameters given in the Table III

| $E_p$<br>GeV | Ejectile      | $\beta$ | $T$<br>MeV | $\sigma$<br>mb | $B/d$ | $F$    | $\chi^2$ |
|--------------|---------------|---------|------------|----------------|-------|--------|----------|
| 1.2          | $p$           | 0.136   | 36.7       | 1400           | 11.4  | 0.63   | 27.2     |
|              | $d$           | 0.160   | 39.1       | 190            | 12.1  | [0.63] | 9.5      |
|              | $t$           | 0.073   | 21.5       | 87             | 4.5   | [0.63] | 2.9      |
|              | $^3\text{He}$ | [0.073] | [21.5]     | 0.44           | 18    | [0.63] | 4.5      |
|              | $^4\text{He}$ | 0.070   | 19.0       | 49             | 6.2   | [0.63] | 13.5     |
| 1.9          | $p$           | 0.160   | 40.7       | 1950           | 11.9  | 0.69   | 46.5     |
|              | $d$           | 0.155   | 41.1       | 330            | 19.0  | [0.69] | 15.3     |
|              | $t$           | 0.066   | 23.8       | 170            | 3.1   | [0.69] | 4.4      |
|              | $^3\text{He}$ | 0.045   | 15.0       | 15.6           | 5.2   | [0.69] | 3.3      |
|              | $^4\text{He}$ | 0.061   | 20.9       | 110            | 4.7   | [0.69] | 15.1     |
| 2.5          | $p$           | 0.156   | 41.7       | 2720           | 12.0  | 0.73   | 39.0     |
|              | $d$           | 0.130   | 42.3       | 530            | 8.6   | [0.73] | 10.5     |
|              | $t$           | 0.050   | 23.3       | 300            | 5.7   | [0.73] | 3.2      |
|              | $^3\text{He}$ | 0.037   | 20.5       | 54             | 5.8   | [0.73] | 2.7      |
|              | $^4\text{He}$ | 0.051   | 20.7       | 210            | 3.7   | [0.73] | 11.5     |

ball" contribution to the spectra increases significantly both, with the decrease of the scattering angle and with the increasing of the beam energy.

Success of description of proton spectra by microscopic model of intranuclear cascade with coalescence of nucleons and evaporation of protons from equilibrated target residuum combined with phenomenological contribution from the "fireball" emission shows that the same method of data description might be applicable for other LCP's.

It is natural to scale the model coalescence contribution to spectra of complex LCP's by the same factor "F" which was used for the proton spectra because the coalescence emission of complex particles is determined by the yield of nucleons leaving the nucleus after intranuclear cascade of collisions.

The fits of parameters characterizing the "fireball" to the experimental spectra of deuterons, tritons,  $^3\text{He}$ , and  $^4\text{He}$  were therefore performed with the same scaling factors of coalescence and evaporation emission as those for the proton spectra: 0.63, 0.69, and 0.73 for beam energy 1.2, 1.9, and 2.5 GeV, respectively. Very good description of the experimental data was achieved for all particles with exception of  $\alpha$ -particles for which it was necessary to add a contribution of another moving source - with parameters very close to those used for IMF's. This additional contribution led to perfect description of the  $\alpha$  - particle spectra. Quality of the data reproduction is

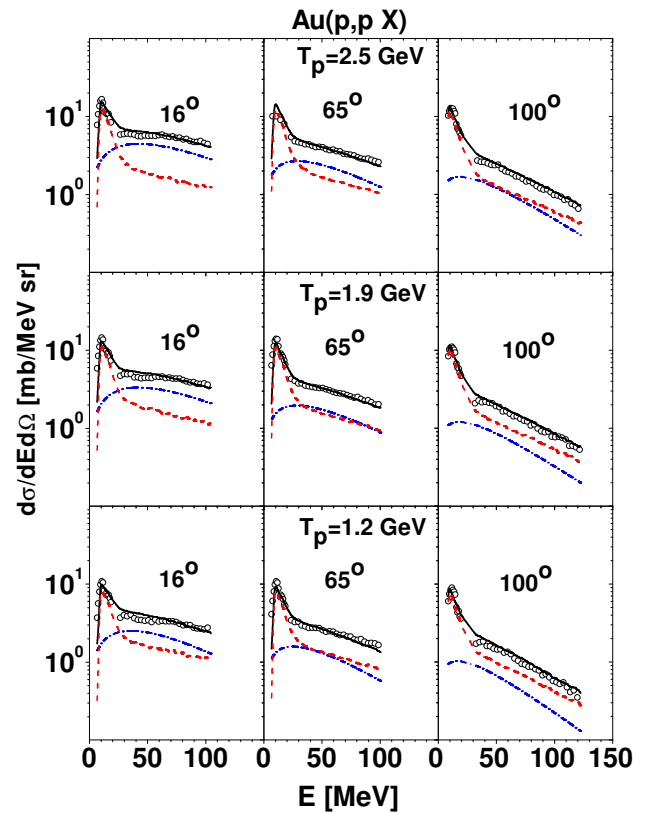


FIG. 5: (Color online) Open circles represent experimental energy spectra of protons measured at selected angles:  $16^\circ$ ,  $65^\circ$ , and  $100^\circ$  (left, central, and right column of the figure, respectively) for three proton beam energies: 1.2, 1.9 GeV – present experiment, and 2.5 GeV – Ref. [1] (lower, central, and upper row of the figure, respectively). The dot-dashed lines present the contribution of proton emission from the "fireball" whereas the dashed lines show calculations made with INCL4.3 plus GEM2 programs. The INCL4.3 plus GEM2 contributions are scaled by the factors 0.63, 0.69, and 0.73 for beam energies 1.2, 1.9, and 2.5 GeV, respectively. The solid lines show sum of all these contributions.

illustrated by Figs. 6, 7, 8, and 9 for deuterons, tritons,  $^3\text{He}$ , and  $^4\text{He}$ , respectively. The parameters of the "fireball" source are listed in the Table II and parameters of additional source used for  $\alpha$ -particles are depicted in the Table III.

As can be seen from the figures, the spectra of deuterons and tritons could not be described, even qualitatively, by coalescence and evaporation of particles alone. The reason of this fact is difference between angular variation of the experimental spectra and those evaluated from the microscopic model. For example, multiplication of coalescence spectra by factor which allows to well reproduce spectrum at  $100^\circ$  still leads to underestimation of the cross sections at smaller angles. On the contrary, adding the contribution of emission of deuterons and tritons from the "fireball" improves the

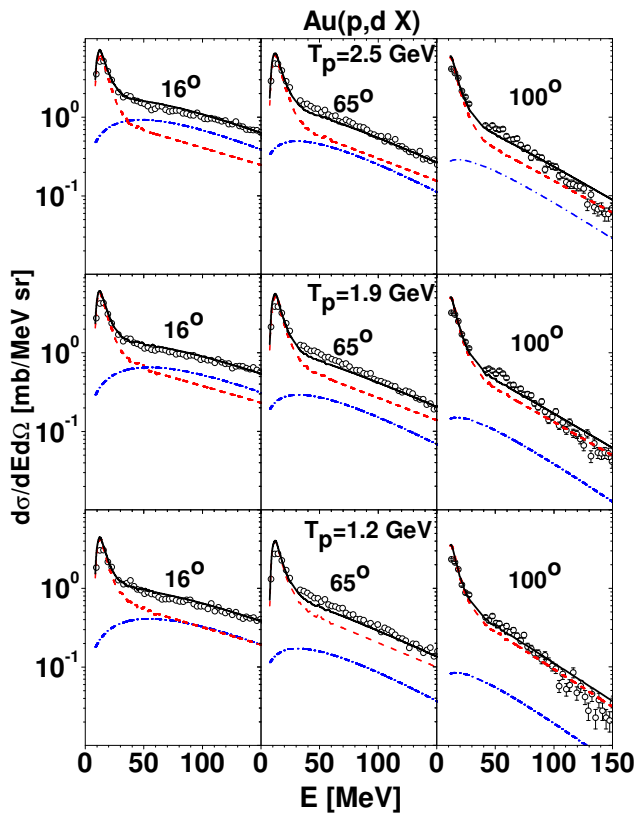


FIG. 6: (Color online) Same as Fig. 5, but for deuterons.

description significantly because this contribution has exactly such an angular and energy dependence which added to microscopic model spectra assures reproduction of the experimental data.

A different situation is present for  ${}^3\text{He}$  channel, where the "fireball" contribution seems to be almost negligible, especially at lower beam energies. It means, that the coalescence together with small evaporation contribution exhaust almost fully the experimental yield of particles leaving no room for the "fireball" emission. It should be, however, emphasized that this very good data reproduction by the coalescence and evaporation mechanisms was obtained after scaling of the theoretical cross sections from INCL4.3+GEM2 by the same factors as those used for the theoretical cross sections for proton emission, thus the presence of "fireball" emission influences also indirectly the description of  ${}^3\text{He}$  emission.

Still another reaction mechanism seems to be responsible for the  $\alpha$ -particle production. The shape as well as magnitude of the experimental spectra for  ${}^3\text{He}$  and  ${}^4\text{He}$  is quite different, showing that evaporation of  $\alpha$ -particles from excited target residuum after intranuclear cascade of nucleon-nucleon collisions is much more abundant than corresponding evaporation of  ${}^3\text{He}$  particles. However, the peak present in the experimental spectra of  ${}^4\text{He}$  is

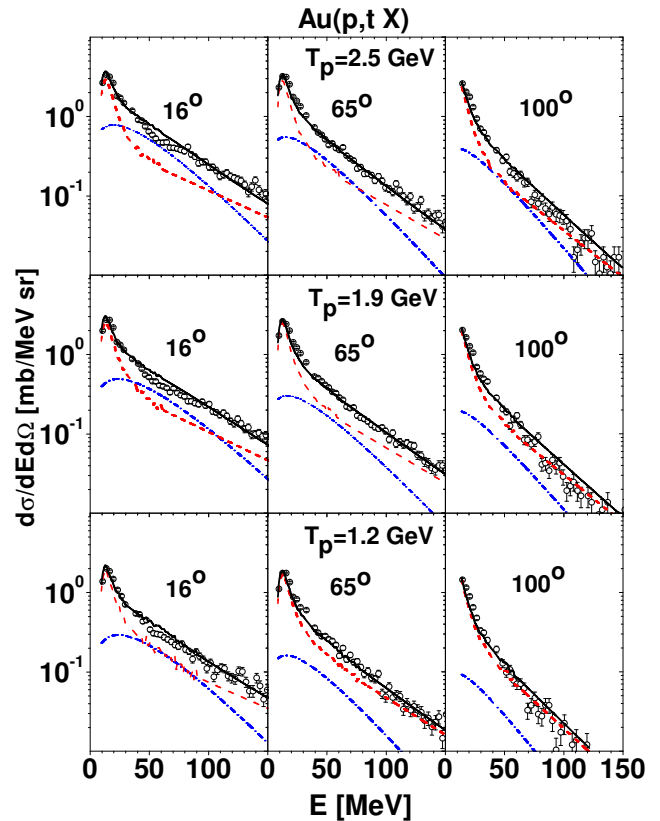


FIG. 7: (Color online) Same as Fig. 5, but for tritons.

much broader than that predicted by evaporation from heavy target residuum. Since neither coalescence mechanism nor "fireball" emission can produce such a peak in the spectrum, thus, another contribution is necessary to reproduce the shape of the peak in the experimental spectra. The naturally appearing solution is to take into consideration the contribution from the moving source of the mass larger than the "fireball" but smaller than heavy target residuum. Such a source, moving faster than target residuum but slower than the "fireball", was observed in the analysis of spectra for all IMF's, thus it is not astonishing that also  $\alpha$ -particle spectra are modified by its contribution.

#### IV. DISCUSSION

The temperature of the "fireball" fitted to describe LCP's data varies only slightly with the beam energy. Its values listed in the Table II do not change more than  $\sim 10\%$  for each ejectile in the beam energy range from 1.2 to 2.5 GeV. This is also true for the temperature of the additional source necessary to be included for good description of  $\alpha$ -particle data and for temperatures of both phenomenological sources applied for parametriza-



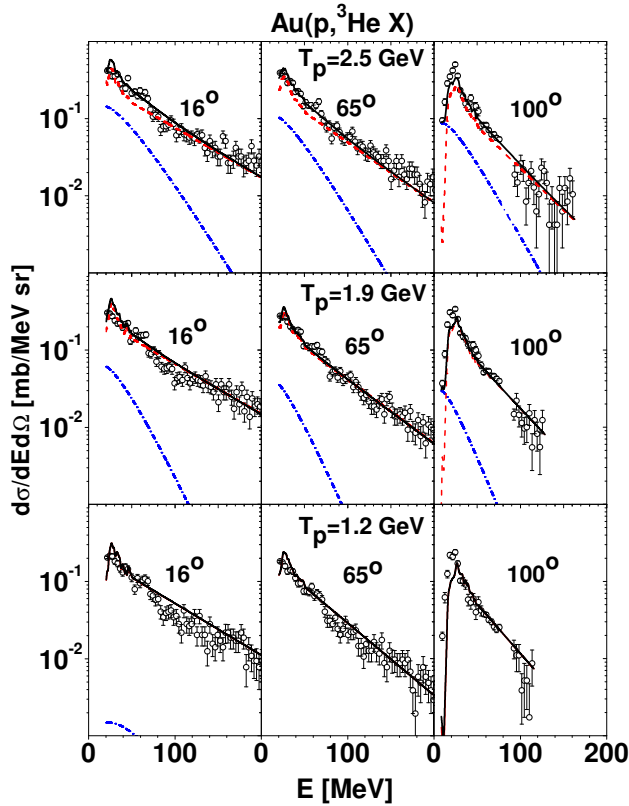


FIG. 8: (Color online) Same as Fig. 5, but for  ${}^3\text{He}$ .

tion of IMF's data. This fact allows to study dependence of the beam energy averaged temperature on the ejectile mass instead temperature dependencies for individual beam energies. Beam energy averaged temperatures of all moving sources are depicted in the lower part of Fig. 10 as function of the ejectile mass  $A$ . It is seen that temperatures of two sources emitting IMF's are grouped into two sets: the full dots - representing slow sources - lie along solid horizontal line  $T = 11.1$  MeV whereas the open circles - representing fast sources - are spread around the dashed line  $T = 30.6 - 1.61A$  MeV. The same procedure applied to apparent temperatures of the "fireball" emitting LCP's shows that the mass dependence of this temperature may be described by linear function:  $T = 49.9 - 8.24A$  MeV (dash dotted line in Fig. 10).

If the ejectile mass  $A$  dependence of the apparent temperature  $T$  of the source is caused only by recoil of the source during emission of registered ejectiles then it is possible to estimate mass of the source  $A_S$  and its true temperature  $\tau$  from parameters of the linear dependence  $T(A)$ . For the fast source emitting IMF's the source temperature is equal to  $\tau = 30.6$  MeV and mass of it is equal to  $A_S = 30.6/1.61 \equiv 19$  nucleons. The temperature of the slow source is independent of the IMF's mass what means that the recoil effect is negligible, i.e. the source is very heavy and its temperature is equal to apparent temper-

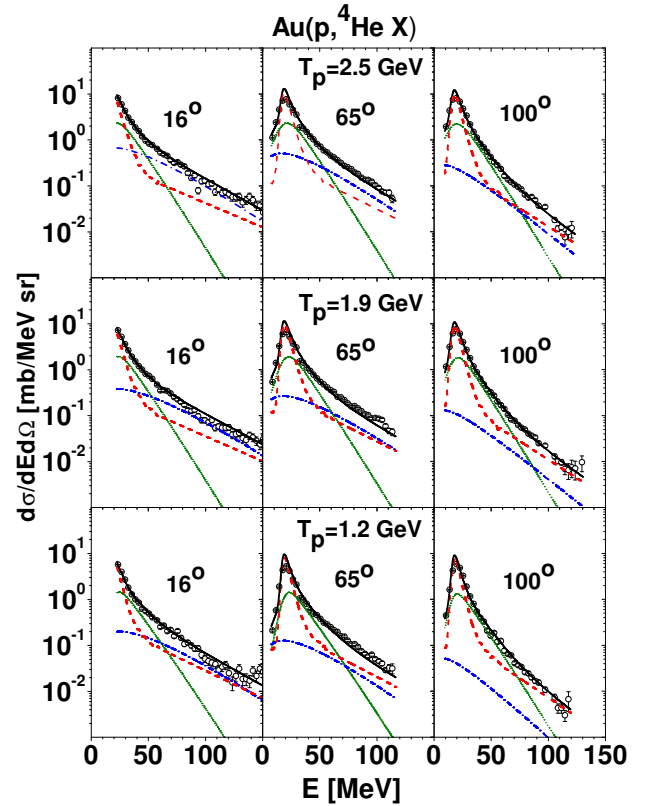


FIG. 9: (Color online) Same as Fig. 5, but for  $\alpha$ -particles. The thin dotted line depicts contribution from fast moving source of the mass intermediate between the "fireball" and the heavy target residuum.

ature found in the fit ( $\tau = 11.1$  MeV). The temperature of "fireball" extracted from the parameters of the fitted straight line is equal to  $\tau = 49.9$  MeV and the "fireball" is built of  $A_S = 49.9/8.24 \equiv 6$  nucleons.

These conclusions seem to be compatible with results of pure phenomenological analysis of two moving sources performed in our previous investigation of LCP's and IMF's for Au+p collisions at proton beam energy 2.5 GeV [1]. In this study the temperature of the slow source for IMF's was  $\sim 12$  MeV, the temperature of the fast source for IMF's was  $\sim 33$  MeV, and the temperature of "fireball" was estimated to be  $\sim 62$  MeV. Mass of the slow source must be very large - close to the mass of the target - because apparent temperature of this source did not vary significantly with the product mass, i.e. recoil could be neglected. The mass of the fast source was equal to mass of  $\sim 20$  nucleons and mass of the "fireball" was close to the mass of  $\sim 8$  nucleons.

The largest deviation between previous results and those found in the present work concern properties of the "fireball". This is not surprising because the "fireball" of the present work is responsible only for a part of the effect which was attributed to the "fireball" in the

TABLE III: Parameters of the intermediate mass source needed to describe well the  $\alpha$  - particle spectra by combination of microscopic model coalescence and evaporation contributions, the "fireball" and intermediate mass source contributions. Parameters  $\beta$ ,  $T$ , and  $\sigma$  have the same meaning as that given in Table II for the "fireball". The  $k$  parameter is the height of the Coulomb barrier in units of simple barrier height estimation by Coulomb potential of two uniformly touching spheres with the charge of the target nucleus and the charge of the emitted particle with radii parameterized as  $R=1.44 A^{1/3}$ .

| $E_p$<br>GeV | $k$             | $\beta$             | $T$<br>MeV     | $\sigma$<br>mb |
|--------------|-----------------|---------------------|----------------|----------------|
| 1.2          | [0.8]           | 0.0094              | 10.6           | 385            |
| 1.9          | $0.83 \pm 0.03$ | $0.0062 \pm 0.0010$ | $10.2 \pm 0.3$ | $577 \pm 23$   |
| 2.5          | $0.80 \pm 0.04$ | $0.0047 \pm 0.0011$ | $10.2 \pm 0.4$ | $764 \pm 38$   |

previous study. However, inspection of Fig. 10 shows also another effect: The straight dashed line representing apparent temperature of the fast source with the mass of about 19 nucleons - found from analysis of IMF's data - crosses the dash dotted line representing apparent temperature of the "fireball" at mass of ejectile  $A \sim 3$ . It means that the temperature parameter of the "fireball" and that of the intermediate mass source are the same for tritons,  ${}^3\text{He}$ , and  ${}^4\text{He}$ . Moreover, the velocity of the "fireball" emitting tritons,  ${}^3\text{He}$ , and  ${}^4\text{He}$  is very close to velocity of the fast source emitting IMF's as it is shown in the upper part of Fig. 10 where the beam energy averaged values of the velocity parameter are collected for IMF's (open circles for the fast source and solid, horizontal line - fixed at velocity of heavy residuum from intranuclear cascade - for the slow source) and for LCP's (full squares for the "fireball" and the full triangle for additional source necessary for description of the  $\alpha$ -particles). Thus, it is not clear whether it is allowed to extract mass of the "fireball" from mass dependence of the apparent temperature of the source fitted to proton, deuteron, triton, and  ${}^{3,4}\text{He}$  data or it is necessary to assume that the source for particles with mass 3 and 4 is identical with the intermediated mass source ( $A_S \sim 19$ ) found for IMF's. If this is the case, then the *genuine* "fireball" contributes mainly to emission of protons and deuterons, thus it is reasonable to conjecture that the mass of the "fireball" should be very light (3-4 nucleons).

It is worth to point out that values of temperature and velocity of the additional source introduced to describe the  $\alpha$ -particle emission (triangles in Fig. 10) are very similar to values characterizing the slow, heavy source emitting the IMF's (solid line in Fig. 10).

All these findings agree well with conclusions derived from pure phenomenological analysis of the p+Au data measured at 2.5 GeV proton beam energy [1], which consist in the statement, that nonequilibrium contribution to production of LCP's and IMF's indicates presence of the mechanism similar to fast break up of the target nucleus

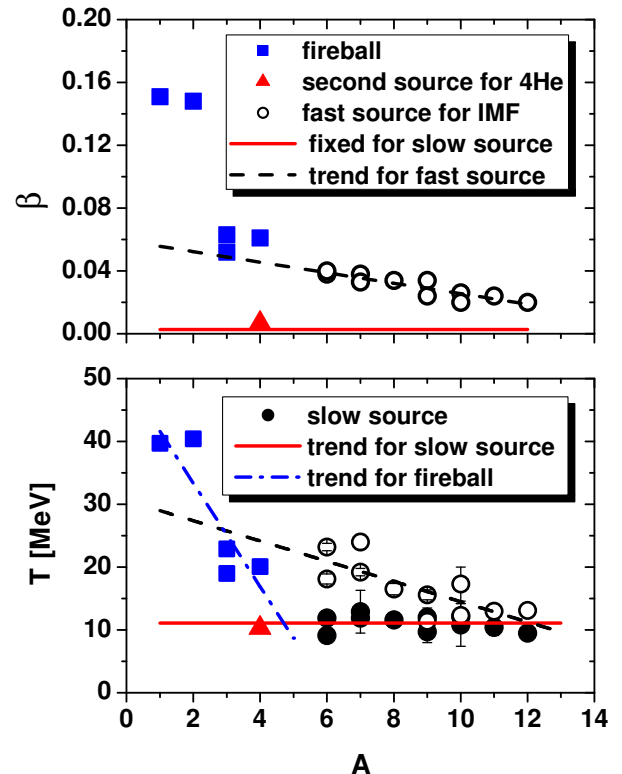


FIG. 10: (Color online) In the *lower part* of the figure the apparent temperature of the moving sources, averaged over beam energies is drawn as a function of the ejectile mass. Open circles and full dots represent values of parameters obtained from analysis of IMF's data for fast and slow source, respectively. Full squares depict temperature of the "fireball" fitted to spectra of LCP's together with the contribution of microscopic model of intranuclear cascade, coalescence and statistical evaporation. Full triangle shows the temperature of the second source fitted to spectra of  $\alpha$ -particles. The solid and dashed lines were fitted to the points representing IMF's and extrapolated to smaller masses. Dash dotted line was fitted to LCP's temperatures of the "fireball". In the *upper part* of the figure the dependence of the beam energy averaged velocity of the sources is drawn versus mass of ejectiles. The symbols have the same meaning as for the lower part of the figure with one exception: The full dots are not shown because the velocity of slower source was fixed during analysis (at velocity of heavy residuum of target nucleus after intranuclear cascade) and it is represented by solid line in the figure. The dashed line was fitted to open circles representing velocities of fast source for IMF's. The line was extrapolated to lower mass region.

in which three moving sources of ejectiles are created. The new result of the present work is an observation that the nonequilibrium emission of LCP's is mediated by two competing mechanisms: surface coalescence of outgoing nucleons and the contribution from three moving sources appearing as result of the break up.

TABLE IV: Cross sections (in millibarns) for production of LCP's by intranuclear cascade and coalescence mechanism (left part of the table), and by the evaporation (right part of the table) - evaluated with INCL4.3 + GEM2 computer programs and scaled by appropriate factors: 0.63, 0.69, and 0.73 for beam energies 1.2, 1.9, and 2.5 GeV, respectively.

| $\bar{E}_p$<br>GeV | coalescence |     |     |               |               | evaporation |     |     |               |               |
|--------------------|-------------|-----|-----|---------------|---------------|-------------|-----|-----|---------------|---------------|
|                    | p           | d   | t   | $^3\text{He}$ | $^4\text{He}$ | p           | d   | t   | $^3\text{He}$ | $^4\text{He}$ |
| 1.2                | 2213        | 613 | 198 | 75            | 62            | 633         | 272 | 134 | 10.2          | 718           |
| 1.9                | 2740        | 771 | 254 | 101           | 80            | 932         | 432 | 212 | 20.4          | 914           |
| 2.5                | 3084        | 859 | 285 | 116           | 90            | 1094        | 526 | 257 | 27.1          | 1019          |

It is interesting to compare cross sections for inclusive LCP's production originating from these two nonequilibrium mechanisms. Values of cross sections for nonequilibrium processes are listed in the Tables II, III and IV, for emission from the "fireball", for emission from additional, slower source, and from coalescence, respectively. Proton beam energy dependence of these cross sections as well as dependence of relative contribution of the "fireball" emission are presented in Fig. 11. Several important conclusions can be derived from inspection of the figure:

- Cross sections for all emitted LCP's increase with energy in approximately exponential way, however, this increase is faster for the "fireball" emission (central part of the figure) than for the coalescence mechanism (lower part of the figure).
- Magnitude of the coalescence cross sections decreases strongly with the mass of ejectile - cf. values of the cross sections in the lower part of Fig. 11: squares - for protons, dots - for deuterons, triangles - for tritons, stars connected by straight lines - for  $^3\text{He}$ , and diamonds - for  $\alpha$ -particles. This behavior may be explained by decreasing probability of capture of more and more nucleons by the nucleon escaping from the nucleus.
- The cross sections for two isobars - triton and  $^3\text{He}$  are quite different. The cross section for triton production is approximately two times larger than that for  $^3\text{He}$ . Such a big difference may be related to ratio  $N/Z=1.49$  of Au nuclei and may be additionally enhanced by the fact that coalescence of two neutral particles - neutrons and one charged particle - proton is not influenced by repulsive Coulomb force, whereas coalescence of two protons and one neutron is certainly hindered to some extent by Coulomb interaction. This effect is also visible for "fireball" emission of tritons and  $^3\text{He}$ , moreover, the ratio of triton cross section to  $^3\text{He}$  cross sections is larger than for coalescence and varies (decreases) strongly with beam energy - cf. central part of Fig. 11.
- Relative contribution of "fireball" mechanism in-

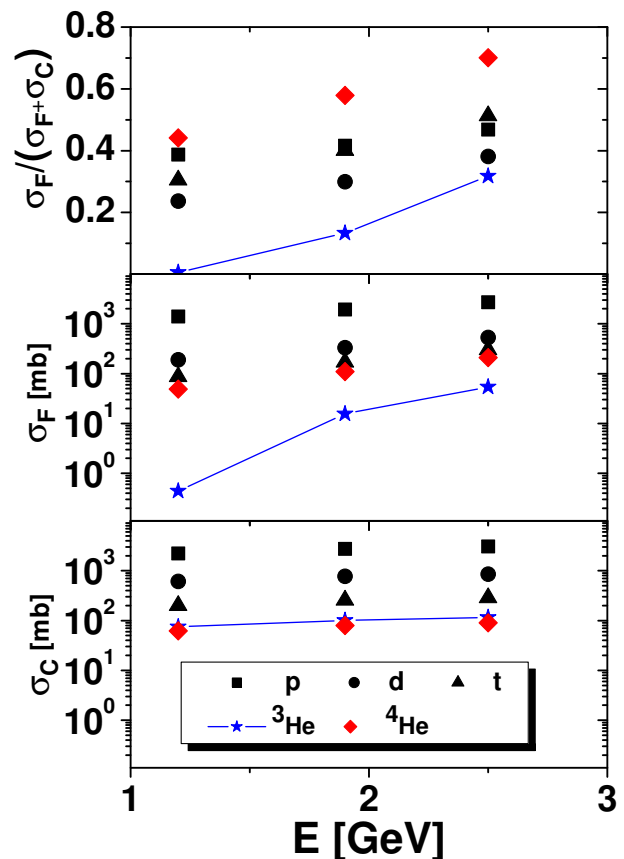


FIG. 11: (Color online) In the upper part of the figure the beam energy dependence of the relative contribution of "fireball" emission to the whole nonequilibrium production cross sections is shown. In the central part of the figure the energy dependence of the cross section due to the "fireball" mechanism and in the lower part of the figure the energy dependence of the production cross sections due to coalescence are depicted. Full squares, dots, and triangles represent proton, deuteron and triton cross sections, respectively. The stars connected by solid line show cross sections for  $^3\text{He}$  production and the diamonds correspond to  $\alpha$ -particle cross sections.

creases almost exponentially with the beam energy - cf. upper part of Fig. 11. Slope of the energy dependence is smallest for protons, has intermediate value for deuterons and tritons, and is largest for  $^3\text{He}$  and  $\alpha$ -particles. It should be, however, pointed out that in spite of such a fast increase of "fireball" emission for both helium isotopes, the contribution of this mechanism is less important for these particles than for the hydrogen isotopes. For  $^3\text{He}$  this is caused by the fact that relative contribution of "fireball" emission is small - smaller than 20% of the sum of both considered mechanisms, and furthermore, it manifests itself only at forward angles and small energies (cf. Fig. 8). Thus,  $^3\text{He}$  spectra can be quite well reproduced by scaled co-

alescence mechanism contribution alone. For the  $\alpha$ -particles, the "fireball" contribution is comparable to that of the coalescence mechanism, however, as it was discussed above, another nonequilibrium process gives large contribution to the experimental spectra: emission from the source of mass intermediate between the "fireball" and the heavy target residuum created in the fast stage of the reaction.

The present investigations allowed to find the beam energy variation of the contribution of nonequilibrium processes to the studied emission of LCP's. In Fig. 12 the ratio is shown of the sum of all nonequilibrium processes, i.e., the "fireball" emission and the coalescence for p, d, t, and  $^3\text{He}$  ejectiles with additional contribution of the intermediate mass source for  $^4\text{He}$  particles, to sum of all these processes and compound nucleus cross section evaluated by INCL4.3+GEM2 programs and scaled by factors found from the fit to the proton spectra. As can be seen from the figure the contribution of nonequilibrium processes is very large for all energies. It has the largest values (over 80 %) for  $^3\text{He}$  and for protons. For deuterons and tritons this contribution is about 70 %, whereas for  $\alpha$ -particles it is the smallest, however, still quite large (40 - 50 % - depending on the beam energy). The important conclusion is that the energy dependence of the relative contribution of nonequilibrium processes is very weak with the exception of the  $\alpha$ -particles, where this relative contribution increases by 20% from the lowest beam energy to the highest one. Such - almost constant - value of the contribution of nonequilibrium processes seems to be rather unexpected in view of strong increase of the total production cross sections in the studied, broad range of the beam energy. However, it may be explained by the fact that cross sections of both, equilibrium and nonequilibrium processes, increase with energy in similar manner.

## V. SUMMARY AND CONCLUSIONS

Double differential cross sections  $d^2\sigma/d\Omega dE$  were measured for p, d, t,  $^3,4,6\text{He}$ ,  $^6,7,8,9\text{Li}$ ,  $^7,9,10\text{Be}$ , and  $^{10,11,12}\text{B}$  produced in collisions of 1.2 and 1.9 GeV protons with Au target. It was found that the spectra measured at 16, 20, 35, 50, 65, 80, and 100 degrees in the present experiment as well as such data obtained at 2.5 GeV beam energy [1] are very similar indicating large contribution of nonequilibrium processes. The data for IMF's were analyzed in the frame of phenomenological model of two moving sources emitting isotropically the ejectiles. The slow source simulated evaporation of particles from the equilibrated remnant of the intranuclear cascade of nucleon-nucleon collisions whereas the fast source was responsible for description of nonequilibrium processes. Very good reproduction of all cross sections was achieved with the parameters which vary smoothly with the beam

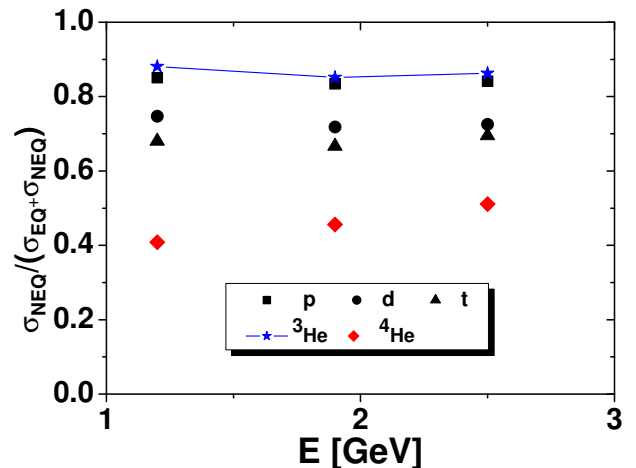


FIG. 12: (Color online) The ratio of the sum of cross sections for nonequilibrium processes (the coalescence and "fireball" emission cross sections for protons, deuterons, tritons, and  $^3\text{He}$  particles, whereas for  $\alpha$ -particles still cross section for emission from intermediate mass source is added) to sum of cross sections for all these processes and cross section for emission from the equilibrated target residuum after intranuclear cascade is shown as function of beam energy. The cross sections evaluated by programs INCL4.3+GEM2 were multiplied by factors 0.63, 0.69, and 0.73 for beam energies 1.2, 1.9, and 2.5 GeV, respectively. The same symbols are used as in Fig. 11, i.e., full squares present results for protons, full dots - results for deuterons, triangles - correspond to tritons, stars connected by solid line depict the  $^3\text{He}$  data and full diamonds represent  $\alpha$ -particles.

energy and mass of ejectiles. It was found that the cross sections corresponding to both sources increase with the energy and the relative contribution of the nonequilibrium processes varies from  $(27 \pm 3)\%$  at 1.2 GeV beam energy to  $(44 \pm 5)\%$  at 2.5 GeV beam energy.

The LCP's data were analyzed by means of the microscopic model which takes into consideration the intranuclear cascade of nucleon-nucleon collisions, coalescence of the nucleons escaping from the nucleus after the cascade, and the evaporation of particles from the equilibrated, excited residuum of the target nucleus. The calculations were performed using the computer program INCL4.3 of Boudard et al. [7] for intranuclear cascade and coalescence processes, and by GEM2 computer program of S.Furihata [9],[10] for evaporation. It should be emphasized that free parameters of both models have been not fitted to the data but original values of these parameters, recommended by the authors, have been used. Model cross sections were significantly smaller than the experimental data for emission of protons with energies larger than  $\sim 30$  MeV whereas the evaporation contribution, which dominates the smaller energy range of spectra, overestimates the data. The discrepancy increases with increasing beam energy and with decreasing the emission

angle.

It was assumed that an additional contribution to the microscopic model cross sections has to be added to account for the observed discrepancies in the description of proton data. The isotropic emission of particles from the "fireball" moving forward, i.e., in the direction parallel to the beam, leads to desirable energy and angular distributions. Thus, this process has been taken into consideration for improving the proton data description. Parameters of the "fireball" were treated as free parameters. The magnitude of the contribution from microscopic model was allowed to be scaled down because of two reasons: (i) in the intranuclear cascade model it is assumed that *each* proton bombarding the nucleus initiates the cascade of nucleon-nucleon collisions, thus, "fireball" process, which consists in creation of *a correlated group* of the nucleons emitted in the forward direction, is completely neglected, (ii) the magnitude of the coalescence process may be modified by variation of the conditions which determine whether nucleons form the cluster or move independently.

Excellent description of the proton spectra was achieved for all emission angles and for all beam energies with the parameters of the "fireball" varying smoothly with the beam energy. Furthermore, the factor which was used to scale down the contribution from intranuclear cascade modified by coalescence and the contribution of the evaporation was almost energy independent: 0.63, 0.69, and 0.73 for beam energy 1.2, 1.9, and 2.5 GeV respectively.

The spectra of other LCP's were analyzed in the same manner, i.e., the microscopic model contribution (coalescence and evaporation cross sections) was multiplied by the same factor which was used for the proton channel and parameters of the "fireball" were fitted independently for each ejectile and each beam energy. Excellent description of all data has been obtained with smoothly varying parameters of the "fireball". The data for  ${}^4\text{He}$  channel still need inclusion of the contribution from another slow moving source.

The contribution of the "fireball" mechanism to the nonequilibrium processes is quite significant for all light charged particles (20% - 60% - depending on the particles and beam energy). Magnitude of this contribution increases almost exponentially with the beam energy.

Rather astonishing result of the present investigation, that the relative contribution of all nonequilibrium processes to the total cross sections (40% - 80%, depending on the particles) remains almost energy independent for all light charged particles is caused by presence of similar energy dependence for both, equilibrium and nonequilibrium processes in the studied energy range. Such a weak energy dependence of the relative contribution of nonequilibrium processes was also found for production of intermediate mass fragments, as it was stated above.

Comparison of parameters of moving sources used in description of IMF's and LCP's data at three proton energies; 1.2, 1.9 and 2.5 GeV confirms our hypothesis pos-

tulated in Ref. [1], which claims that the proton impinging on the Au target interacts with group of nucleons lying on its straight way through the nucleus what leads to emission of a "fireball" consisted of several nucleons. The excited remnant nucleus may decay into two prefragments which manifest themselves as moving sources of LCP's and IMF's, whereas the "fireball" emits only LCP's. It was found in the present analysis that the parameters of the "fireball" fitted to spectra of tritons,  ${}^3\text{He}$  and for  $\alpha$ -particles are very similar to parameters of the light source emitting IMF's. Therefore, it seems that the *genuine* "fireball" contributes mainly to emission of protons and deuterons and, thus, it is consisted of 3 - 4 nucleons. Then the lighter prefragment (of mass of  $\sim 19$  nucleons), appearing as result of decay of excited remnant, is responsible for emission of tritons,  ${}^3\text{He}$  and  $\alpha$ -particles. The spectra of  $\alpha$ -particles show also large contribution originating from the larger prefragment, i.e. from the emission of slow source responsible for IMF's production.

These findings are in agreement with observations made for hadron production in high energy (of order of 50 - 200 GeV) proton-nucleus collisions [11],[12],[13] where the reaction does not proceed on the total nucleus of mass  $A$  but the bombarding proton interacts with *the effective target* consisted of several nucleons;  $\sim 0.7A^{0.31}$  [12]. For the Au target such an effective target would have a mass of 3.6 nucleons, what fits well with estimated mass of the fireball of the present study and justifies identification of the "fireball" with the "effective target". Furthermore, the deep spallation process of production of  ${}^{149}\text{Tb}$ , studied by Winsberg *et al.* [14] in proton - Au collisions at energies 1 - 300 GeV was also explained by Cumming [15] assuming manifestation of the effective target with the mass of  $(3.1 \pm 0.4)$  nucleons for proton energies larger than  $\sim 2$  GeV. This mass again agrees with the "fireball" mass found in our investigations and confirms proposed interpretation of the "fireball".

It is worth to point out that the observation of the effective target was also reported in production of heavy fragments in proton - U collisions at proton energies 11.5 GeV [16] ( $A=140-210$ ), [17] ( $A=131$ ), and light fragments at 11.5 - 400 GeV [18] ( ${}^{44}\text{Sc}$  -  ${}^{48}\text{Sc}$ ), as well as IMF's (with  $Z=3-14$ ) in proton - Xe collisions at 1 - 19 GeV energies [19].

The presence of heavier sources accompanying the "fireball" and mechanism of their creation was predicted and discussed in Refs. [2], [20], [21], and [22] as result of "cleavage" of the excited remnant nucleus into two excited prefragments after "fireball" emission. In our analysis these heavier prefragments manifest themselves as two sources emitting IMF's as well as tritons,  ${}^3\text{He}$  and  $\alpha$ -particles. Their contribution to proton and deuteron spectra is not pronounced, thus it seems, that the proton and deuteron spectra are dominated by emission from fireball (large ejectile energies) and by evaporation from heavy target residuum (small ejectile energies).

In summary, our investigations lead to a consistent

picture of reaction mechanism responsible for nonequilibrium processes, in which the proton impinging on the target can either initiate cascade of binary nucleon-nucleon collisions accompanied by surface coalescence of nucleons into LCP's or interacts coherently with a group of nucleons leading to emission of three excited groups of nucleons; the "fireball" and two heavier prefragments with different masses. All three excited groups of nucleons are sources of ejectiles. Present investigation shows, that the presence of the effective target and - in consequence - the fast break up mechanism, manifests itself at proton beam energies 1.2 - 2.5 GeV, lower than those from previous studies, quoted to above.

The important conclusion of the present study is the statement, that for good description of the double differential cross sections for all LCP's it is necessary to assume competition of two mechanisms of the nonequilibrium processes: coalescence of nucleons escaping from the nucleus after intranuclear cascade of nucleon-nucleon collisions and isotropic emission of LCP's from the fast source - "fireball" - moving forward along the beam direction. A need to introduce presence of the "fireball" contribution seems to indicate that the lack of correla-

tion between nucleons, inherent in intranuclear cascade models, leads to oversimplified microscopic description of the reaction mechanism. Thus, the realistic microscopic model has to take this effect into consideration.

### Acknowledgments

We acknowledge gratefully the fruitful discussions on the coalescence mechanism with A.Boudard, J.Cugnon, and S. Leray as well as providing us with new version of INCL4.3 computer program. The technical support of A.Heczko, W. Migdał, and N. Paul in preparation of experimental apparatus is greatly appreciated. This work was supported by the European Commission through European Community-Research Infrastructure Activity under FP6 "Structuring the European Research Area" programme (CARE-BENE, contract number RII3-CT-2003-506395 and Hadron Physics, contract number RII3-CT-2004-506078) as well as the FP6 IP-EUROTRANS FI6W-CT-2004-516520.

- 
- [1] A. Bubak, A. Budzanowski, D. Filges, F. Goldenbaum, A. Heczko, H. Hodde, L. Jarczyk, B. Kamys, M. Kistryn, St. Kistryn, *et al.*, Phys. Rev. C **76**,014618 (2007)
  - [2] J. Aichelin, J. Hüfner, and R. Ibarra, Phys. Rev. C **30**, 107 (1984)
  - [3] G.D. Westfall, J. Gosset, P.J. Johansen, A.M. Poskanzer, W.G. Meyer, H.H. Gutbrot, A. Sandoval and R.Stock, Phys. Rev. Lett. **37**, 1202 (1976)
  - [4] R. Barna, V. Bollini, A. Bubak, A. Budzanowski, D. D.Pasquale, D. Filges, S. V. Förtsch, F. Goldenbaum, A. Heczko, H. Hodde, *et al.*, Nucl. Instr. Meth. in Phys. Research A **519**, 610 (2004)
  - [5] A. Boudard, J. Cugnon, S. Leray, and C. Volant, Phys. Rev. C **66**, 044615 (2002)
  - [6] A. Letourneau, A. Böhm, J. Galin, B. Lott, A. Péghaire, M. Enke, C. M. Herbach, D. Hilscher, U. Jahnke, V. Tishchenko, *et al.*, Nucl. Phys. A **712**, 133 (2002)
  - [7] A. Boudard, J. Cugnon, S. Leray, and C. Volant, Nucl. Phys. A **740**, 195 (2004)
  - [8] G. D. Westfall, R. G. Sextro, A. M. Poskanzer, A. M. Zebelman, G. W. Butler, and E. K. Hyde, Phys. Rev. C **17**, 1368 (1978)
  - [9] S. Furihata, Nucl. Instr. and Meth. in Phys. Research B **71**, 251 (2000)
  - [10] S. Furihata and T. Nakamura, Journal of Nuclear Science and Technology Supplement **2**, 758 (2002)
  - [11] G. Berlad, A. Dar, and G. Eilam, Phys. Rev. D **13**, 161 (1976)
  - [12] C. Halliwell, J. E. Elias, W. Busza, D. Luckey, L. Votta, and C. Young, Phys. Rev. Lett. **39**, 1499 (1977)
  - [13] Meng Ta-chung and E. Moeller, Phys. Rev. Lett. **41**, 1352 (1978).
  - [14] L. Winsberg, M.W. Weisfield, and D. Henderson, Phys. Rev. C **13**, 279 (1976)
  - [15] J.B.Cumming, Phys. Rev. Lett. **44**, 17 (1980)
  - [16] B. D. Wilkins, S. B. Kaufman, E. P. Steinberg, J. A. Urbon, and D. J. Henderson, Phys. Rev. Lett. **43**, 1080 (1979).
  - [17] S. Biswas and N. T. Porile, Phys. Rev. C **20**, 1467 (1979)
  - [18] D. R. Fortney and N. T. Porile, Phys. Rev. C **21**, 2511(1980)
  - [19] N. T. Porile, A. J. Bujak, D. D. Carmony, Y. H. Chung, L. J. Gutay, A. S. Hirsch, M. Mahi, G. L. Paderewski, T. C. Sangster, R.P. Scharenberg, and B. C. Stringfellow, Phys. Rev. C **39**, 1914 (1989)
  - [20] M. A. Cirit and F. Yazici, Phys. Rev. C **23**, 2627 (1981)
  - [21] S. Bohrmann, J. Huefner and M.C. Nemes, Phys. Letters 120B, 59 (1983)
  - [22] J. Hüfner, H. M. Sommermann, Phys. Rev. C **27**, 2090 (1983)